Tribo-Mechanical Properties of DLC Coatings Deposited on Nitrided Biomedical Stainless Steel

Rony Snyders, Etienne Bousser, Philippe Amireault, Jolanta E. Klemberg-Sapieha,* Eunsung Park, Kate Taylor, Kevin Casey, Ludvik Martinu

Diamond-like carbon (DLC) coatings are frequently considered for biomedical applications due to their attractive tribo-mechanical properties combined with good biocompatibility. In the present work, DLC coatings have been deposited on 316L stainless steel (SS) substrates. The duplex approach consisted of surface nitriding in a radio frequency (RF) discharge for the reinforcement of SS-DLC bonding prior to DLC deposition (0.5 μm thick). Chemical composition and morphology of the nitrided SS were assessed by XPS and SEM, while depth-sensing indentation, ball-on-flat tribometry, and microscratch testing were used to determine the tribo-mechanical performance of the nitrided SS and of DLC coated SS samples. We found that the formation of a thick (∼1–2 μm), hard (15 GPa) metal nitride layer at the SS surface has a strong influence on enhancing the coating adhesion (critical load of 6.5 N) and wear resistance of DLC (wear factor 3–8 $\times 10^{-8}$ $mm^3 \cdot N^{-1} \cdot m^{-1}$ compared to 10^{-5} $mm^3 \cdot N^{-1} \cdot m^{-1}$ for nitrided SS).

Introduction

Diamond-like carbon (DLC) is assigned to a large variety of amorphous carbon-based materials containing from 1% (a-C) to 50% (a-C:H) of hydrogen and a high fraction of sp^3 hybridized carbon (from 50% for a-C:H to 85% for a-C).[1,2] DLC coatings exhibit excellent physico-chemical and tribo-mechanical properties such as high electrical resistivity, optical transparency, impermeability, high hardness, wear resistance, and a low friction coefficient.[3,4] Moreover, they provide high corrosion resistance due to the inertness of C and H as the main constituents.[3,5]

This combination of properties makes DLC an excellent candidate for use in medical implants and tools.[1,2,5] In particular, those exposed to severe wear environments such as artificial knees, hips, and femoral heads.[3,5,6] In the latter case, the bulk material is usually made of a metal [stainless steel (SS), CoCr, or Ti-based alloys], while the acetabular cup is usually made of ultra high molecular weight polyethylene (UHMWPE).[7] The main limitation of prosthesis lifetime is the production of UHMWPE wear particles which can cause severe tissue reaction.[6] Indeed, it has been found that the linear wear of the UHMWPE cup is 0.1–0.2 $mm \cdot year^{-1}$, and it increases after 10 years of use.[6] As a result, coating the femoral head with DLC is expected to solve many of such problems.

Despite much progress, rather contradictory results have been reported on the efficiency of DLC coatings for reducing wear of the UHMWPE counterpart. Certain authors claim a decrease of wear by a factor of

R. Snyders, E. Bousser, P. Amireault, J. E. Klemberg-Sapieha, L. Martinu
Department of Engineering Physics, École Polytechnique de Montréal, Box 6079, Station "Centre ville", Montreal, Quebec, Canada H3C 3A7
E-mail: jsapieha@polymtl.ca
E. Park, K. Taylor, K. Casey
Medtronic, Inc., 710 Medtronic Parkway, Minneapolis, MN 55432-5604, USA

Plasma Process. Polym. **2007**, *4*, S640–S646
© 2007 WILEY-VCH Verlag GmbH & Co. KGaA, Weinheim
DOI: 10.1002/ppap.200731601

10–100,[6] while others do not observe any influence of the DLC coatings on the wear behavior.[8] The discrepancy in these results can be attributed to numerous issues, primarily to film properties and deposition methods, but also to the liquid lubricant used during tribological testing, and to the surface texture of the tested samples.[9] It has been demonstrated that even single scratches on the DLC surface can increase the UHMWPE counterpart wear rate by a factor of 30–70.[9]

A major issue in this type of applications is the adhesion between the "hard" DLC coating and the "soft" plastic[10] or metallic substrate. Important effort must therefore be made in order to improve the interface between the two components. Numerous papers have recently reported the influence of surface pre-treatment of the metallic substrate before DLC deposition. This includes ion bombardment,[11,12] homogeneous[13] or graded[14,15] interlayers and plasma nitriding as part of the so-called duplex method[16] leading to important improvements of DLC adhesion. Nevertheless, these methods are rather complex and require sophisticated experimental arrangements.

In the present work, we address two issues described above, namely the adhesion enhancement of DLC coatings on 316L biomedical stainless-steel (SS) substrates by plasma nitriding and its effect on the tribo-mechanical properties of the subsequently deposited DLC coatings. Our goals are (i) to study the efficiency of a "simple" plasma nitriding process so as to improve adhesion of the DLC on SS, and (ii) to compare the tribological performance of the DLC against different materials, namely Al_2O_3, SS, and UHMWPE.

Experimental Part

SS substrate pre-treatment as well as DLC deposition were performed in a turbomolecularly pumped radio frequency (RF, 13.56 MHz) PECVD system equipped with a 20 cm diameter RF powered electrode where a self-induced DC bias voltage, V_B, develops. After polishing, the 316L SS substrates were ultrasonically cleaned in 1,1-dichloroethylene (15 min), ethanol (5 min), and acetone (5 min), and introduced into the chamber. After pumping for 1 h, the substrates were plasma cleaned for 15 min in an Ar discharge, using the conditions reported in Table 1. The subsequent nitriding process in pure N_2 RF plasma was performed for different durations ($t_N = 1$–8 h), while keeping all other parameters constant (see Table 1). Finally, DLC films were deposited for 30 min without intentional heating, using a 10 sccm Ar/40 sccm CH_4 mixture with a total working pressure (p_{tot}) of 100 mTorr and $V_B = -300$ V. The thickness of the DLC coating was evaluated by both spectroscopic ellipsometry and profilometry, and it was around 0.5 μm for all the samples.

XPS analyses were performed in a VG-ESCALAB 3 Mark II system. Survey spectra were recorded with 50 eV pass energy, while the high resolution spectra in the regions of interest (Fe2p and Cr2p lines) were acquired with 20 eV pass energy. Shirley-type background subtraction was used prior to peak separation of unsmoothed XPS spectra. Chemical shift (ΔBE) and full width at half maximum (FWHM) of the different lines of Cr and Fe species are reported in Table 2 along with the corresponding chemical bonds. ΔBE of the $2p_{3/2}$ lines as well as the energy difference between the $2p_{3/2}$ and $2p_{1/2}$ lines (ΔE) agree with the published values. During the fitting procedure, α_3 and α_4 satellite lines as well as shake-up lines (only for the Fe_2O_3 and FeO species) were also taken into account. For Mg K_α radiation, the energetic positions of α_3 and α_4 satellite lines with respect to the $2p_{1/2}$ line are, respectively, −8.4 and −10.1 eV, with intensities of 8 and 4% of the corresponding $2p_{1/2}$ line.[18] In the case of shake-up lines, energetic positions, with respect to the $2p_{3/2}$ line, were +7.1 and +8.7 eV, respectively.[25] The curve fitting quality was evaluated by the chi-square convergence.

Hardness (H) and Young's modulus (E) were determined by depth-sensing indentation using the Hysitron Triboindenter® equipped with a Berkovich tip in agreement with the ISO 14577-1 Standard.[26] The data were processed using the Hysitron software providing load–displacement curves corrected for thermal drift and machine constants (frame compliance, transducer spring force, and electrostatic force constants). Load–displacement plots were analyzed according to the Oliver–Pharr method[27] by fitting a power law relationship to the unloading curve and determining the initial unloading stiffness. For each sample, H and E were obtained from 100 indentations with applied loads ranging from 100 to 10 000 μN, while the penetration depth ranged between 20 and 200 nm depending on the sample.

A computer-controlled microscratch tester (MST®, CSEM, Neuchâtel, Switzerland), equipped with an acoustic emission detector and a CCD camera, was used to evaluate the adhesion between DLC and SS. A Rockwell C indenter with a radius of 200 μm was used to scratch the samples mounted on a motorized test table. Scratch length was constant at 10 mm, and the applied load was linearly increased at a rate of 10 $N \cdot min^{-1}$. The value of the

Table 1. Experimental conditions for sample pre-treatment, nitriding, and DLC deposition.

Step	Discharge pressure, p_{tot}	Gaseous mixture	Bias, V_B	Duration, t	Sample labeling
	mTorr		V		
Etching	200	10 sccm Ar	−800	15 min	SS
Nitriding	200	50 sccm N_2	−500	1 h → 8 h (i)	SS/N_i
DLC deposition	100	10 sccm Ar/40 sccm CH_4	−300	30 min	SS/N_i/DLC

© 2007 WILEY-VCH Verlag GmbH & Co. KGaA, Weinheim

Table 2. Assignment of the lines observed in the high resolution XPS spectra, chemical shift (ΔBE), energy difference between $2p_{1/2}$ and $2p_{3/2}$ lines (ΔE), and FWHM, compared to literature data.

XPS peak	Species	Oxidation state	Δ*BE* (eV) from this work/literature [ref]	Δ*E* (eV) [ref]	FWHM (eV) [ref]
$Cr2p_{3/2}$	Cr metallic	0	574.6/574.2 [17]	9.2 [18]	2.5 [18]
	Cr_2N	1+	576.2/576.1 [18]	9.4	2.1
	CrN	2+	576.2/576.8 [19]	9.4	2.1 [18]
	$Cr(OH)_3$	3+	577.2/577.3 [20]	9.8	3.5 [18]
	CrO_2	4+	576.1/576.3 [21]	9.8	3.0
$Fe2p_{3/2}$	FeN	+2	707.7/707.1 [17]	13.3	2.2 [18]
	FeO	+2	709.8/709.8 [22]	13.6	2.8 [18]
	Fe_2O_3	+2,+3	711.1/710.8 [23]	13.6 [17]	4.0 [18]
	FeO(OH)	+3	712.2/711.8 [24]	13.6	4.0

critical load, at which first cracking failure occurs (L_{C1}), was determined from both the acoustic signal and by optical microscopy. Five scratch tests were realized on each sample.

Tribological performance and wear of the samples were evaluated using a reciprocating ball-on-flat test [Figure 3(b)] in dry conditions. Different balls of 4.76 mm in diameter (SS, Al_2O_3 and UHMWPE) were loaded against SS, SS/N_i, and SS/N_i/DLC samples (where i represents the nitriding duration in hours). Reciprocating sliding with an average sliding velocity of 10 $cm \cdot s^{-1}$ and a stroke length of 1 cm was induced by the relative linear displacement of the ball during 30 min. The normal force applied during the test was 22.2 N. After completion of the test, the wear volume of the balls (V) was evaluated by measuring the worn part of the ball with a micrometer. The wear tracks on the samples were characterized by performing profilometry scans in perpendicular direction, from which the wear factor (W) was calculated as[28]

$$W = \frac{V_t}{PX} [mm^3 \cdot N^{-1} \cdot m^{-1}] \quad (1)$$

Here, V_t is the wear volume of the track, X the sliding distance, and P the load. The coefficient of friction (μ) was continuously recorded during the test; the values reported here refer to μ after 20 min of the wear test.

Results and Discussion

Characterization of Nitrided SS

In the first part of this study, we focus on the evaluation of the chemical structure of SS substrates after plasma exposure. While other elements are also present (e.g., Mo, Mn, and Co), XPS measurements reveal that Cr and Fe are the main metallic species composing the surface of the 316L SS (Table 3). Therefore, we studied in more detail the influence of t_N on these species. Figure 1 shows the restructuring of both Cr2p and Fe2p lines after 8 h of nitriding. Before plasma treatment, Cr and Fe species are mostly oxidized (6.2 and 52.5%, respectively) and hydroxilyzed (93.8 and 47.5%, respectively) (Table 4). Indeed, the components of the Cr2p and Fe2p lines are mainly attributable to $Cr(OH)_3$ (577.2 eV) and CrO_2(576.1 eV), and to FeO(OH) (712.2 eV) and Fe_2O_3 (711.1 eV),

Table 3. XPS quantification of SS nitrided samples from broad scans.

Composition	C	O	N	Mo	Mn	Co	Cr	Fe
	at.-%	at.-%	at.-%	at.-%	at.-%	at.-%	at.-%	at.-%
SS	30.8	49.6	0.0	0.4	2.3	3.9	6.8	6.2
SS/N_1	31.1	35.0	19.4	0.2	1.1	3.1	4.1	6.0
SS/N_3	27.1	20.0	32.1	0.3	1.4	3.7	6.2	9.2
SS/N_5	26.3	26.3	28.9	0.2	0.5	2.4	6.3	8.1
SS/N_8	19.6	19.6	30.7	0.5	0.6	4.6	12.0	12.8

© 2007 WILEY-VCH Verlag GmbH & Co. KGaA, Weinheim
DOI: 10.1002/ppap.200731601

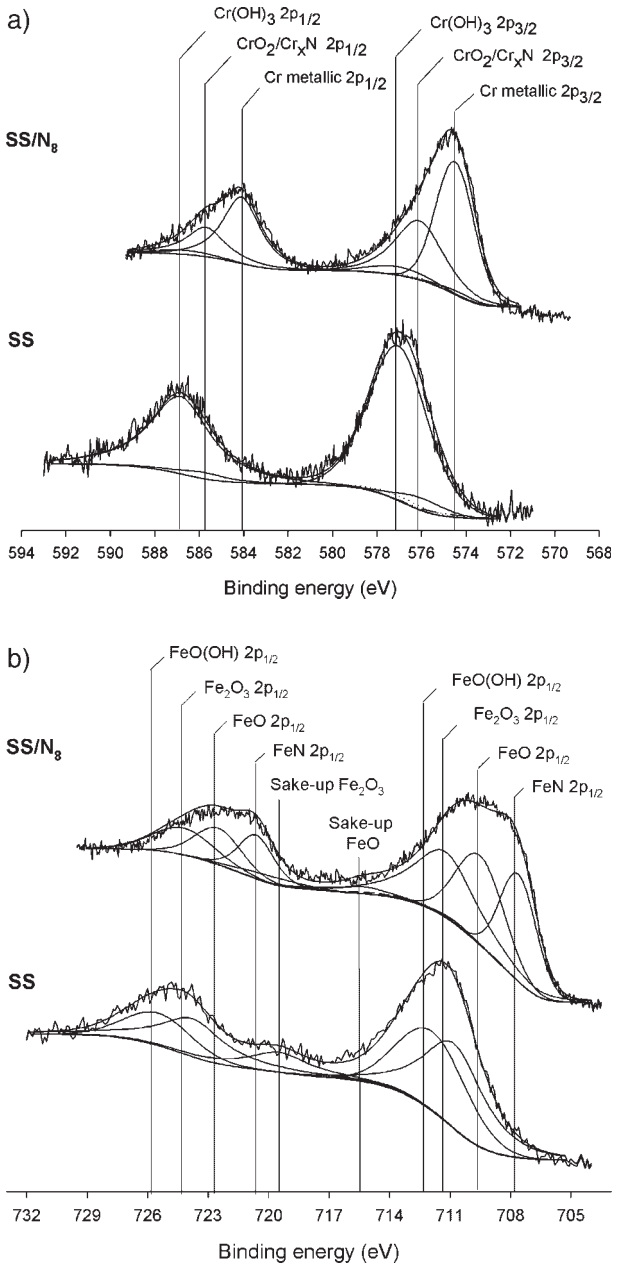

Figure 1. Deconvolution of the Cr2p (a) and Fe2p (b) XPS lines for SS and SS/N_8 samples.

respectively. After 8 h of nitriding, the lines are completely restructured and shifted toward lower binding energies suggesting a reduction of the SS surface as also supported by the decrease of the oxygen content to 19.6 at.-% (Table 3).

After nitriding, the Cr2p line [Figure 1(a)] reveals three effects: (i) appearance of metallic Cr (574.6 eV) which becomes the main specie contributing to the Cr2p line, (ii) important decrease of the $Cr(OH)_3$ line, and (iii) an increase of the line attributed to CrO_2 (Table 2). The increase of the CrO_2 line appears surprising considering the plasma-induced surface reduction pointed out above. However, taking into account the overlapping CrO_2 (576.1 eV) and CrN/Cr_2N (576.2 eV) lines, we believe that the increase of the feature at 576.2 eV is related to the formation of nitrogen-containing Cr species on the SS surface.

The behavior of the Fe2p line [Figure 1(b)] after 8 h of nitriding is similar to that of the Cr line. Indeed, the FeO(OH) line at 712.2 eV disappears while other lines attributed to FeO and FeN appear at 709.8 and 707.7 eV, respectively. We also observe a decrease of the Fe_2O_3 line at 711.1 eV. These results confirm the reduction and nitriding of the SS surface. It should be noted that even after 8h of nitriding, we did not observe any metallic iron at 706.9 eV.[17]

Table 4 reports the evolution of the atomic fraction of the different components contributing to both Cr2p and Fe2p lines as a function of t_N. In both cases, we observe a stabilization of surface composition after approximately 3 h of nitriding. Moreover, we clearly observe that the overall hydroxyl species are affected by the nitriding process. These results suggest formation of nitrided chromium (Cr_xN) and of both oxidized and nitrided iron species (FeO, FeN). Therefore, we conclude that plasma nitriding leads to surface reduction, mainly by removing hydroxyl species, and to formation of nitrided species. This is supported by the broad scan results (Table 3) which show a decrease of [O] from 49.6 to 19.6 at.-%, and to an increase of [N] from 0 to 30.7 at.-% after 8 h nitriding.

The nitrided samples were further evaluated for their mechanical properties. Example of hardness as a function of depth obtained for SS (reference) and SS/N_3 (3 h of nitriding) are shown in Figure 2. We obtained $H \approx 6$ GPa for SS while after 3 h of nitriding, H exhibits a maximum of 14 GPa for indentation depths (h_c) between approximately

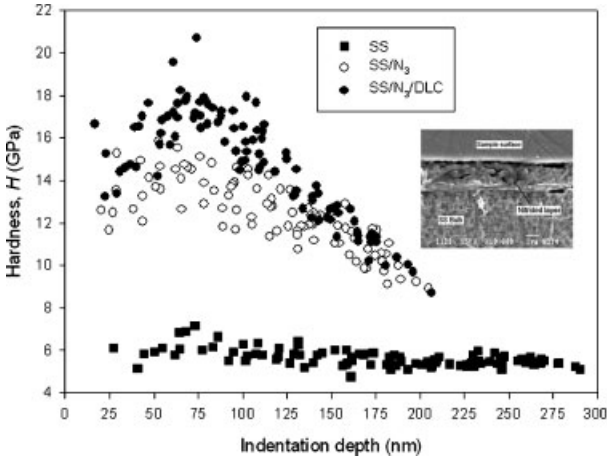

Figure 2. Nanohardness measurements of SS, SS/N_3, and SS/N_3/DLC samples and SEM cross-sectional image of an SS/N_3/DLC sample.

© 2007 WILEY-VCH Verlag GmbH & Co. KGaA, Weinheim

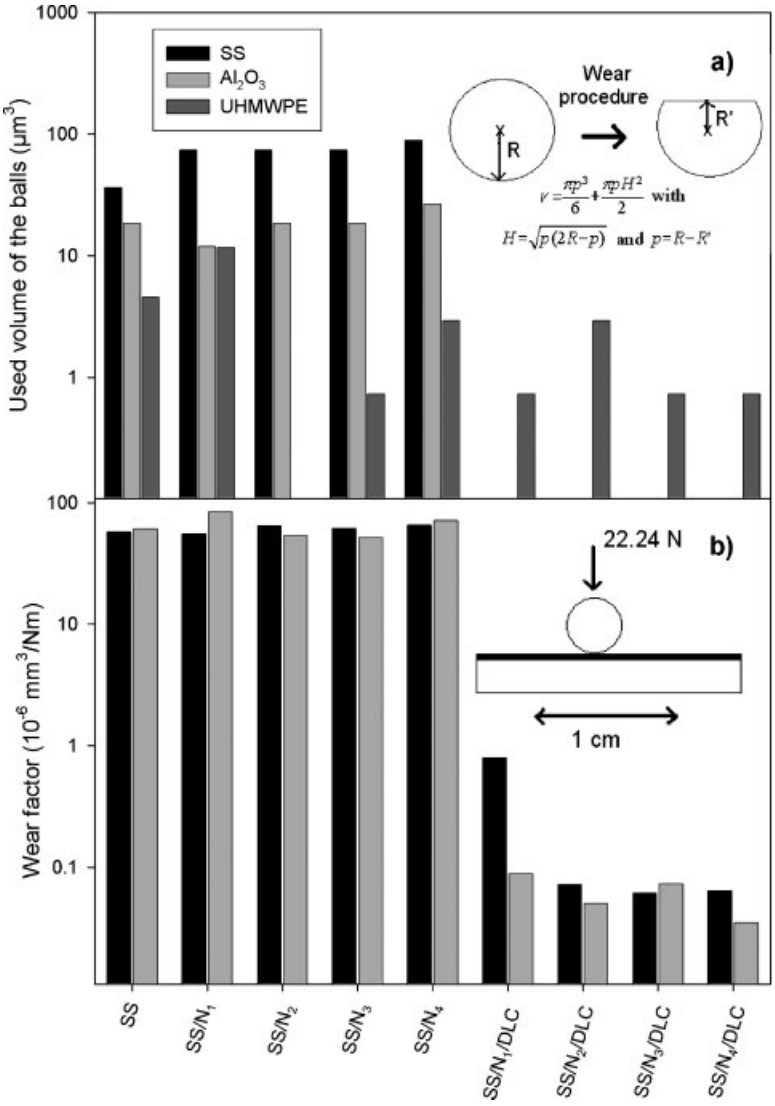

Figure 3. Wear characteristics of balls (a) and of SS, SS/N_i, and SS/N_i/DLC samples (b) after the wear testing.

50 and 125 nm. For $h_c < 50$ nm, surface roughness and indenter tip effects lead to a decrease of the measured hardness, while for $h_c > 125$ nm, the measurement is influenced by the SS bulk. The latter behavior is common and thus it is widely accepted that H of a coating is measured from indentations with penetration depths not exceeding 5–10% of the total coating thickness, where substrate effects are negligible.[29] The high value of H is attributed to the nitrided layer formed after plasma treatment that is about 2 μm thick as verified by SEM cross-sectional microscopy for SS/N_3 (Figure 2). H values measured for other t_N are similar to the one of SS/N_3 (Table 3). In addition, E does not vary with t_N and, it presents values close to 220 GPa for all of the analyzed samples (Table 3). We conclude that t_N influences the thickness of the modified layer but not its properties.

Tribo-Mechanical Properties of the DLC Coatings

After plasma nitriding, the SS/N_i substrates were covered by a 0.5 μm thick DLC and the influence of t_N on the tribo-mechanical properties was studied (Table 5). Using the micro-scratch test, we observe an important increase of L_{C1} as a function of t_N. Indeed, no adhesion was observed for untreated SS ($L_{C1} = 0$), while L_{C1} stabilizes around 6.5 N for SS/N_3. This is consistent with XPS results for which we also observed surface composition stabilization for 3 h of treatment (Table 4). The L_{C1} values determined in this work are comparable to the ones reported elsewhere for comparable film thickness. For example, Podgornik et al.[30] reported L_{C1} values varying between 2 and 4 N for ta-C deposited on duplex-treated AISI 4140 steel.

For well adhering DLC films ($L_{C1} > 6$), the H and E do not vary with t_N (Table 5). Their values, close to $H = 18$ GPa and $E = 140$ GPa, are in agreement with other published results for DLC.[1,3,31]

The tribological tests particularly focused on the evaluation of DLC deposited for $t_N = 1$–4 h, since the most significant modifications occurred for $0 < t_N < 3$ h. In Figure 3(a), we report the wear volume of the balls, V, for different ball materials used in this work. For SS and SS/N_i samples, we observe a clearly higher V for SS balls ($40–90 \times 10^6$ μm^3) than for Al_2O_3 ($\approx 20 \times 10^6$ μm^3) and UHMWPE ($1–11 \times 10^6$ μm^3) balls. For SS and Al_2O_3 balls, V yields similar results for different tested samples; however, a larger scatter of the values is observed for UHMWPE balls. A smaller wear of alumina balls compared to SS can be attributed to a lower intrinsic hardness of the latter material. While UHMWPE has a lower hardness than SS and Al_2O_3, a lower V has nevertheless been found. This can possibly be attributed to the lack of wear particles generated by UHMWPE on DLC, thus maintaining a purely adhesive type of wear compared to the adhesive/abrasive mechanism for both SS and alumina counter materials. When the nitrided substrates are covered by DLC, virtually no wear of the SS and Al_2O_3 balls is observed, while the wear of the UHMWPE balls is almost constant for all SS/N_i/DLC samples ($1–2 \times 10^6$ μm^3). These results clearly

© 2007 WILEY-VCH Verlag GmbH & Co. KGaA, Weinheim
DOI: 10.1002/ppap.200731601

Table 4. XPS quantification and tribo-mechanical properties (hardness, Young's modulus, and friction coefficient) of SS nitrided samples.

XPS quantification		SS	SS/N_1	SS/N_3	SS/N_5	SS/N_8
%						
Cr	Cr	0	30.5	41.6	42.0	58.0
	$CrN/Cr_2N/CrO_2$	6.2	34.6	38.9	42.9	36.4
	$Cr(OH)_3$	0.93.8	34.9	19.5	15.1	5.6
Fe	FeN	0	37.8	27.6	38.8	37.4
	FeO	0	30.7	50.2	40.6	40.3
	Fe_2O_3	5.25	31.5	22.2	20.6	22.3
	FeO(OH)	4.	0	0	0	0
Mechanical properties						
Hardness, *H* (GPa)		≈6	≈14	≈15	≈16	≈15
Elastic modulus, *E* (GPa)		≈220	≈220	≈220	≈220	≈220
Friction coefficient, μ		SS	SS/N_1	SS/N_2	SS/N_3	SS/N_4
Al_2O_3		0.12	0.11	0.22	0.12	0.13
SS		0.10	0.12	0.12	0.16	0.13
UHMWPE		0.23	0.21	0.20	0.18	0.20

underline the significant role of DLC in maintaining the integrity of the SS and Al_2O_3 counterpart materials compared to UHMWPE. This can be explained by the formation of a transfer layer in the case of an SS or Al_2O_3 balls, while in the case of UHMWPE, formation of the transfer layer is not clear.[9]

Figure 3(b) shows the evolution of *W* for different tested samples. First, we do not observe any wear of the samples when using UHMWPE balls, most probably due to low hardness of the polymer compared to the DLC counterpart. Using SS and alumina balls, we observe important and similar *W* for SS and the nitrided samples ($5–8 \times 10^{-5}$ $mm^3 \cdot N^{-1} \cdot m^{-1}$). However, when the nitrided samples are coated with DLC, *W* decreases significantly to values ranging from 3 to 8×10^{-8} $mm^3 \cdot N^{-1} \cdot m^{-1}$ for all tested SS/N_i/DLC samples. This demonstrates the major effect of the DLC on the wear resistance of SS, an observation in agreement with data in the literature. For example, Podgornik et al.[30] reported *W* between 0.1 and 1×10^{-6} $mm^3 \cdot N^{-1} \cdot m^{-1}$ for DLC coated SS samples against SS balls, while Ronkainen et al.[32] reported *W* of 3×10^{-8} $mm^3 \cdot N^{-1} \cdot m^{-1}$ for DLC against alumina.

Analysis of the friction coefficient (μ) for all samples (SS, nitrided SS, and DLC coated SS) reveals higher values for UHMWPE balls than for SS or Al_2O_3 balls (Table 4 and 5). μ determined for SS and Al_2O_3 balls against SS and SS/N_i are similar and close to 0.12. However, when SS is covered with DLC, μ decreases to 0.05 for Al_2O_3 balls and to 0.09 for SS balls. For UHMWPE balls we observe a decrease of μ with t_N from 0.23 for untreated SS down to 0.18–0.20 for the various nitrided SS samples. However, unlike Al_2O_3 and SS balls, no important differences were found between SS/N_4 and DLC coated samples. These measurements underline the known lubricant effect of DLC coatings[1] which has

Table 5. Tribo-mechanical properties (critical load, hardness, Young's modulus and friction coefficient) of DLC coatings deposited on SS and nitrided samples.

Mechanical properties	SS/N_1/DLC	SS/N_2/DLC	SS/N_3/DLC	SS/N_4/DLC	SS/N_5/DLC	SS/N_8/DLC
Hardness, *H* (GPa)	≈18	–	≈18	–	≈16	≈18
Young modulus, *E* (GPa)	≈140	–	≈140	–	≈140	≈140
Critical load, L_{C1} (N)	5.2 ± 0.2	–	6.3 ± 0.1	–	6.5 ± 0.2	6.7 ± 0.8
Friction coefficient, μ						
Al_2O_3	0.14	0.10	0.09	0.05	–	–
SS	0.14	0.10	0.11	0.09	–	–
UHMWPE	0.15	0.18	0.18	0.20	–	–

© 2007 WILEY-VCH Verlag GmbH & Co. KGaA, Weinheim

been observed for both SS and Al_2O_3 balls but not for UHMWPE. As mentioned above the absence of a transfer layer between UHMWPE and DLC, suggested in the literature,[10] can explain this behavior. The values determined in the present work are comparable to the ones previously published. For example, Ronkainen et al.[32] reported μ of an Al_2O_3 ball against DLC between 0.07 and 0.09, depending on the characteristics of DLC coating (a-C, a-C:H, and a-C:H + Ti), while Platon et al.[33] reported μ of DLC coated SS balls on UMHWPE close to 0.25.

Conclusion

We studied tribo-mechanical properties of DLC coatings deposited in an RF discharge onto low pressure RF plasma nitrided 316L biomedical SS. Through detailed XPS analysis of the nitrided SS surface, we determined nitriding time-dependent reduction of the Fe and Cr oxides and hydroxides followed by subsequent formation of nitrided compounds (Cr_xN and FeN). Nanoindentation measurements, supported by SEM imagery, suggested the formation of a 1–2 μm thick hard nitrided layer. Adhesion evaluation by microscratch testing showed that the nitriding process used in this work resulted in well-adhering DLC on SS ($L_{C1} = 6.5$ N). Moreover, the wear behavior of DLC coated SS, evaluated by ball-on-flat measurements using SS, Al_2O_3, and UMHWPE balls, was greatly improved compared to uncoated SS samples (nitrided or not). The DLC coated samples exhibited improved wear properties: (i) the wear of SS and Al_2O_3 balls is virtually eliminated, although for the UHMWPE balls wear is only weakly diminished, and (ii) the wear of SS samples by SS and Al_2O_3 balls is reduced by three orders of magnitude ($5–8 \times 10^{-5}$ to $3–8 \times 10^{-8}$ $mm^3 \cdot N^{-1} \cdot m^{-1}$). Finally, we observed a significant reduction of the friction coefficients of SS and Al_2O_3 balls on DLC (0.5–0.9 compared to 0.12), and no measurable modifications for UHMWPE balls. Finally, this work demonstrates the possibility, using a "simple" plasma-based nitriding process, to prepare high-performance DLC coatings on SS substrate.

Acknowledgements: The authors wish to thank Professor *Szpunar* and Mr. *M. Aziz* (McGill University) for assistance with tribological testing. R. S. acknowledges the scholarship from the *Belgian National Fund for Scientific Research (FNRS)*. E. B. and P. A. acknowledge scholarships from the *Fonds Québécois de la Recherche sur la Nature et la Technologie*. This work was supported by the *Natural Sciences and Engineering Research Council (NSERC)* of Canada and by *Medtronic, Inc.*

Received: September 25, 2006; Accepted: November 17, 2006; DOI: 10.1002/ppap.200731601

Keywords: diamond-like carbon (DLC); interface engineering; plasma nitriding; stainless steel; tribo-mechanical properties; XPS

[1] A. Grill, *Diamond Relat. Mater.* **1999**, *8*, 428.
[2] L. Martinu, "Amorphous Carbon Film", in: *High Density Technologies in Materials Science*, F. Garbassi, E. Occhielo, Eds., Kluwer Academic Publishers, London 1988.
[3] A.-S. Loir, F. Garrelie, C. Donnet, J.-L. Subtil, M. Belin, B. Forest, F. Rogemend, P. Laporte, *Appl. Surf. Sci.* **2005**, *247*, 22.
[4] A. Raveh, L. Martinu, H. M. Hawthorne, M. R. Wertheimer, *Surf. Coat. Technol.* **1993**, *58*, 45.
[5] F. C. Cui, D. J. Li, *Surf. Coat. Technol.* **2001**, *131*, 481.
[6] V. M. Tiainen, *Diam. Relat. Mat.* **2001**, *10*, 153.
[7] S. Santavirta, Y. T. Konttinen, R. Lappalainen, *Clin. Orthop.* **1999**, *12*, 92.
[8] D. Sheeja, B. K. Tay, X. Shi, S. P. Lau, C. Daniel, S. M. Krishnan, *Diamond Relat. Mater.* **2001**, *10*, 1043.
[9] R. Hauert, *Tribol. Int.* **2004**, *37*, 991.
[10] L. Martinu, in: "*Plasma Processing of Polymers*", R. D'Agostino, P. Favia, F. Fracassi, Eds., Kluwer Academic Publishers, Dordrecht 1997, p. 247.
[11] L. Martinu, A. Raveh, A. Domingue, L. Bertrand, J. E. Klemberg-Sapieha, S. C. Gujrathi, M. R. Wertheimer, *Thin Solid Films* **1992**, *208*(1), 42.
[12] L. Martinu, J. E. Klemberg-Sapieha, O. M. Küttel, A. Raveh, M. R. Wertheimer, *J. Vac. Sci. Technol. A* **1994**, *12*(4), 1360.
[13] C. C. Chen, F. C.-N. Hong, *Appl. Surf. Sci.* **2005**, *243*, 296.
[14] T. Sonoda, A. Watazu, K. Kato, T. Yamada, T. Asahina, *Surf. Interface Anal.* **2004**, *36*, 1144.
[15] K.-L. Choy, E. Felix, *Mater. Sci. Eng.* **2000**, *A278*, 162.
[16] B. Podgornik, J. Vizintin, *Diamond Relat. Mater.* **2000**, *10*, 2232.
[17] E. Menthe, K.-T. Rie, J. W. Schultze, S. Simson, *Surf. Coat. Technol.* **1995**, *74–75*, 412.
[18] J. F. Moulder, W. F. Stickle, P. E. Sobol, K. D. Bomben, in "*Handbook of X-Ray Photoelectron Spectroscopy*", Perkin Elmer Corporation, Eden Prairie 1992.
[19] I. L. Singer, J. S. Murday, *J. Vac. Sci. Technol. A* **1980**, *17*(1), 327.
[20] J. Stypula, J. Stoch, *Corros. Sci.* **1994**, *12*, 2159.
[21] I. Ikemoto, K. Ishii, S. Kinoshita, H. Kuroda, M. A. A. Franco, J. Thomas, *J. Solid State Chem.* **1976**, *17*, 425.
[22] T. L. Barr, *J. Phys. Chem.* **1978**, *82*(16), 1801.
[23] G. Hollinger, G. Marest, H. Jaffrezic, J. Tousset, N. Moncoffre, *Nucl. Instrum. Methods Phys. Res. B* **1985**, *7*(8), 177.
[24] N. S. McIntryre, D. G. Zetaruk, *Anal. Chem.* **1977**, *49*, 1521.
[25] T. J. Chuang, C. R. Brundle, K. Wandelt, *Thin Solid Films* **1978**, *53*, 19.
[26] "*Metallic Materials—Instrumented Indentation Test for Hardness and Materials Parameters—Part 1: Test Method*", International Standard ISO 14577-1, 2002.
[27] W. C. Oliver, G. M. Pharr, *J. Mater. Res.* **1992**, *7*, 1564.
[28] P. Firkins, J. L. Hailey, J. Fisher, A. H. Lettington, R. Butter, *J. Mater. Sci. Mater. Med.* **1998**, *9*, 597.
[29] S. J. Bull, *J. Vac. Sci. Technol. A* **2001**, *19*(4), 1404.
[30] B. Podgornik, J. Vizintin, H. Ronkainen, K. Holmberg, *Thin solid Films* **2000**, *377–378*, 254.
[31] J. Robertson, *Surf. Coat. Technol.* **1992**, *50*, 185.
[32] H. Ronkainen, S. Varjus, K. Holmberg, *Wear* **1998**, *222*, 120.
[33] F. Platon, P. Fournier, S. Rouxel, *Wear* **2001**, *250*, 227.

© 2007 WILEY-VCH Verlag GmbH & Co. KGaA, Weinheim